Full length article

# Nonlinear vibration and dynamic buckling of eccentrically oblique stiffened FGM plates resting on elastic foundations in thermal environment

Seung-Eock Kim[a], Nguyen Dinh Duc[a,b,c,*], Vu Hoai Nam[d], Nguyen Van Sy[b]

[a] National Research Laboratory, Department of Civil and Environmental Engineering, Sejong University, 209 Neungdong-ro, Gwangjin-gu, Seoul 05006, South Korea
[b] Advanced Materials and Structures Laboratory, VNU, Hanoi – University of Engineering and Technology, 144 Xuan Thuy, Cau Giay, Hanoi, Viet Nam
[c] Infrastructure Engineering Program, VNU, Hanoi – Vietnam-Japan University, My Dinh 1, Tu Liem, Hanoi, Viet Nam
[d] University of Transport Technology, 54 Trieu Khuc, Thanh Xuan, Hanoi, Viet Nam

## ARTICLE INFO

## ABSTRACT

This paper presents a semi-analytical approach to investigate the nonlinear dynamic response and vibration of eccentrically oblique stiffened functionally graded plate resting on elastic foundation. The Lekhnitskii's smeared stiffener technique is improved by using a transformation technique for oblique stiffeners. Governing equations are solved by classical shell theory, Galerkin method, stress function with temperature-dependent material effects. The results show the influences of geometrical parameters, material properties, imperfection, the elastic foundations, eccentrically oblique stiffeners, mechanical loads and temperature on the nonlinear dynamic response and nonlinear vibration of plates. The numerical results in this paper are compared with the results reported in other reports.

## 1. Introduction

Eccentrically stiffened functionally graded (FGM) plate and shell are very important structures in engineering design of aircraft, missile and aerospace industries. In recent years, many investigations have been carried out on static and dynamic response of FGM plate and shell with and without stiffeners.

Reddy et al. [1–4] studied analytical static and dynamic application of the plate. By using the extended finite element method and the first order shear deformation theory [2–4] and high order shear deformation plate theory [1,3] to analysis of stress and deflection of plates and cylindrical shells. Arciniega and Reddy [5] researched large deformation analysis of FGM shells, by using the first order shear deformation theory. To study nonlinear bending and post buckling of circular plate under mechanical and thermal loadings, Ma and Wang [6] used high order shear deformation plate theory and shooting method. Matsunaga et al. [7] studied deflection and stress behavior of FGM rectangles subject to mechanical and thermal loads. In this paper, the author has used the high order shear deformation theory and the susceptible moving principles to derive basic equations and then solution by using the power series.

For static stability analysis of FGM plate problems, Eslami et al. [8–14] researched buckling behavior of FGM plates under in-plane compressive loading [8] and thermal buckling of FGM plates [9] by using the classical plate theory. And then they extended research to thick plates and used higher-order shear deformation theory [10,11] and included the imperfections of plate to obtain the critical loads [12–14]. Lanhe [15] studied thermal buckling of thick plate, by using the first order shear deformation theory. Ebrahimi et al. [16] researched a theoretical analysis of smart moderately thick shear deformable annular FGM plates. Taczala et al. [17] presented the nonlinear finite element method for studying the nonlinear stability of FGM plates with reinforced by stiffness for mechanical and thermal loads.

For dynamic stability and vibration analysis of FGM plates, Wang and Jean [18] presented the nonlinear steady-state responses of longitudinally traveling FGM plates in contact with liquid. They [19,20] also studied the nonlinear dynamic thermoelastic response of rectangular FGM plates with longitudinal velocity based on the D'Alembert's principle and large-amplitude vibration of sigmoid FGM thin plates with porosities with decomposed results were authenticated numerically with the flexible step-size fourth-order Runge-Kutta approach. Wang et al. [21] developed the nonlinear dynamics of a translational FGM plate with strong mode interaction and electro-mechanical vibration analysis of FGM piezoelectric porous plates in the translation state [22]. Wang and Jean [23] also investigated the porosity-dependent nonlinear forced vibration analysis of FGM piezoelectric smart

material plates by using both diagnostic and numerical methods and considered vibration behaviors of FGM rectangular plates with porosities and moving in thermal environment [24], the geometric non-linearity was calculated by using von Kármán nonlinear plate theory. Wang et al. [25] studied the nonlinear vibrations of moving FGM plates containing porosities and contacting with liquid: internal resonance. Effects of various parameters on the frequency response of the formation were investigated. Based on the classical plate theory, stress function and Lekhnitskii's smeared stiffeners technique with motion equations with temperature-dependent material properties, Bich et al. [26] considered nonlinear dynamical buckling and vibration of stiffened FGM cylindrical panels. Duc et al. [27,28] studied static buckling and dynamic response of S-FGM circular and elliptic cylindrical shell with three layers of metal - ceramic - metal surrounded by elastic foundation in thermal environment. Duc et al. [29] solved nonlinear thermal stability of eccentrically stiffened FGM truncated conical shells surrounded by elastic foundations and also studied nonlinear vibration and dynamic response of imperfect eccentrically stiffened shear deformable FGM plate in thermal environment in Ref. [30]. Alijani et al. [31] investigated nonlinear vibrations of FGM doubly curved shallow shells. Kolahchi et al. considered dynamic stability analysis of temperature-dependent functionally graded CNT-reinforced visco-plates resting on orthotropic elastomeric medium in Ref. [32], agglomeration effects on the dynamic buckling of viscoelastic microplates reinforced with SWCNTs using Bolotin method in Ref. [33] and comparative study on the bending, vibration and buckling of viscoelastic sandwich nano-plates based on different nonlocal theories using DC, HDQ and DQ methods in Ref. [34]. The nonlinear vibrations of rotating, laminated composite circular cylindrical shells subjected to radial harmonic excitation in the neighborhood of the lowest resonances were investigated by Wang [35] by using the Galerkin and harmonic balance methods. Wang et al. [36] studied the nonlinear vibration of metal foam cylindrical shells reinforced with graphene platelets by using the improved Donnell nonlinear shell theory and different types of porosity and graphene platelet distribution were taken into account. Wang et al. [37] investigated the nonlinear dynamic characteristics of FGM sandwich thin nanoshells conveying fluid incorporating surface stress influence. The velocity potential and Bernoulli's equation were applied to describe the fluid pressure.

To the best knowledge of authors, there are no publications on the vibration and nonlinear dynamic response of the eccentrically oblique stiffened thin FGM plates. This paper presents a semi-analytical approach of nonlinear buckling and vibration of FGM plates reinforced by oblique stiffener system. An improved Lekhnitskii's smeared stiffener technique for oblique stiffeners and Galerkin method are applied to obtain the time-dependent nonlinear equation of motion of plates. Solving this equation is mathematically difficult, therefore, a numerical approach is applied by using the fourth-order Runge-Kutta method to obtain the dynamic response of plates.

## 2. Eccentrically oblique stiffened thin FGM plate rested on elastic foundations

### 2.1. Geometrical and material properties

Consider a ceramic–metal eccentrically stiffened thin FGM plate of length $a$, width $b$, and thickness $h$ resting on elastic foundations. A coordinate system $(x, y, z)$ is established in which $(x, y)$ plane is on the middle surface of the plate and $z$ is the thickness direction $(-h/2 \leq z \leq h/2)$, as shown in Fig. 1. The width and thickness of longitudinal and transversal stiffeners are denoted by $d_x$, $h_x$ and $d_y$, $h_y$ respectively; $s_x$, $s_y$ are the spacing of the longitudinal and transversal stiffeners. The quantities $A_x$, $A_y$ are the cross-section areas of stiffeners and $I_x$, $I_y$, $e_x$, $e_y$ are the second moments of cross-section areas and the eccentricities of stiffeners with respect to the middle surface of plate, respectively. $E_0$, $\alpha_0$ are Young's modulus and the

thermal expansion coefficient of eccentrically stiffeners, respectively.

FGM in this paper is assumed to be made from a mixture of ceramic and metal with the volume-fractions given by a power law

$$V_m(z) = \left( \frac{2z + h}{2h} \right)^N, \quad V_c(z) = 1 - V_m(z), \tag{1}$$

where $N$ is volume fraction index $(0 \leq N < \infty)$, the subscripts $m$ and $c$ refer to the metal and ceramic constituents, respectively. According to the mentioned law, Young's modulus and thermal expansion coefficient can be expressed in the form

$$[E(z, T), \quad \alpha(z, T)] = [E_c(T), \quad \alpha_c(T)] + [E_{cm}(T), \quad \alpha_{cm}(T)] \left( \frac{2z + h}{2h} \right)^N, \tag{2}$$

and the Poisson's ratio $\nu$ is assumed to be a constant and $E_{cm} = E_c - E_m$, $\alpha_{cm} = \alpha_c - \alpha_m$.

It is assumed that the effective properties $Pr_{eff}$ of FGM plate, such as the elastic modulus $E$, the mass density $\rho$ and the thermal expansion coefficient $\alpha$, vary in the thickness direction $z$ are determined by linear rule of mixture as

$$Pr_{eff}(z) = Pr_c V_c(z) + Pr_m V_m(z), \tag{3}$$

in which $Pr$ denotes a material property.

The reaction – deflection relation of Pasternak foundations is given by

$$q = k_1 w - k_2 \nabla^2 w \tag{4}$$

where $\nabla^2 = \partial^2/\partial x^2 + \partial^2/\partial y^2$, $w$ is the deflection of the plate, $k_1$ is Winkler foundation modulus, and $k_2$ is the shear layer foundation stiffness of Pasternak model.

### 2.2. Governing equations

In this study, the classical plate theory is used to derive basic equations to investigate the nonlinear dynamic response and vibration of eccentrically stiffened FGM plate on elastic foundations in thermal environments.

The geometrical compatibility equation for an imperfect FGM plate is written as

$$\varepsilon_{x,yy}^0 + \varepsilon_{y,xx}^0 - \gamma_{xy,xy}^0 = (w_{,xy})^2 - w_{,xx} w_{,yy} + 2w_{,xy} w_{,xy}^* - w_{,xx} w_{,yy}^* - w_{,xx}^* w_{,yy} \tag{5}$$

in which imperfection function $w^*(x, y)$ denotes initial small imperfection of FGM plate.

The nonlinear equilibrium equations of FGM plate are

$$
\begin{aligned}
&N_{x,x} + N_{xy,y} = 0, \\
&N_{xy,x} + N_{y,y} = 0, \\
&M_{x,xx} + 2M_{xy,xy} + M_{y,yy} + N_x w_{,xx} + 2N_{xy} w_{,xy} + N_y w_{,yy} \\
&\quad - k_1 w + k_2(w_{,xx} + w_{,yy}) + q = I_0 w_{,tt} + 2\varepsilon I_0 w_{,t},
\end{aligned} \tag{6}
$$

in which $k_1$ is Winkler foundation modulus, $k_2$ is the shear layer foundation stiffness of Pasternak model, $q$ is an external pressure uniformly distributed on the surface of the plate, $\varepsilon$ is the viscous damping coefficient and

$$I_0 = \sum_{i=1}^{n} \int_{h_{k-i}}^{h_k} \rho(z) dz.$$

The normal strains in the middle surface of the plate taking into account the Von Karman nonlinear terms are given by Ref. [38].
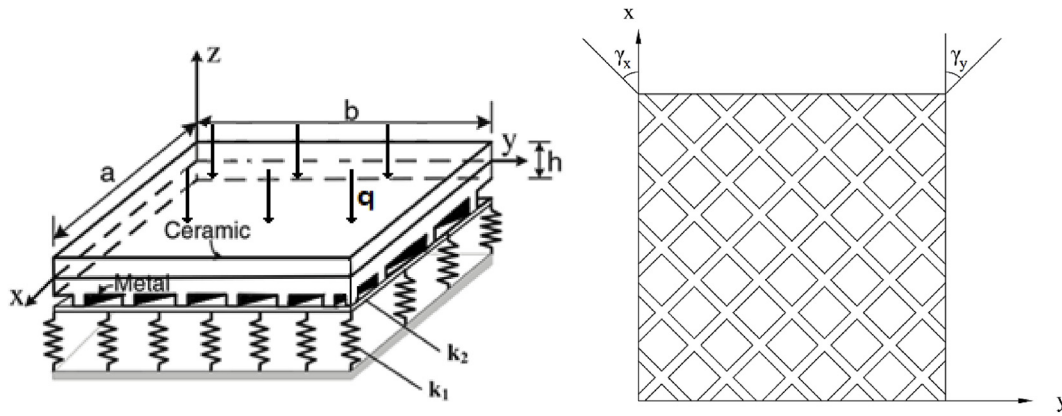
**Fig. 1.** Geometry and coordinate system of an eccentrically oblique stiffened FGM plate resting on elastic foundations.

$$\varepsilon_x^0 = \frac{\partial u}{\partial x} + \frac{1}{2}\left(\frac{\partial w}{\partial x}\right)^2,$$

$$\varepsilon_y^0 = \frac{\partial v}{\partial y} + \frac{1}{2}\left(\frac{\partial w}{\partial y}\right)^2,$$

$$\gamma_{xy}^0 = \frac{\partial u}{\partial y} + \frac{\partial v}{\partial x} + \frac{\partial w}{\partial x}\frac{\partial w}{\partial y}, \tag{7}$$

in which $u$, $v$, $w$ are displacement components corresponding to the coordinates($x$, $y$, $z$),

The strains across the shell thickness at a distance $z$ from the middle surface are

$$\varepsilon_x = \varepsilon_x^0 - z\frac{\partial^2 w}{\partial x^2},$$

$$\varepsilon_y = \varepsilon_y^0 - z\frac{\partial^2 w}{\partial y^2},$$

$$\gamma_{xy} = \gamma_{xy}^0 - 2z\frac{\partial^2 w}{\partial x\partial y}. \tag{8}$$

Hooke's law for a plate is defined as follows

$$\begin{pmatrix}\sigma_x\\\sigma_y\end{pmatrix} = \frac{E}{1-v^2}\begin{pmatrix}\varepsilon_x + v\varepsilon_y\\\varepsilon_y + v\varepsilon_x\end{pmatrix} - (1+v)\alpha\Delta T, \quad (\sigma_{xy}) = \frac{E}{2(1+v)}(\gamma_{xy}), \tag{9}$$

and for the stiffeners is

$$\sigma_\gamma^s = E_0\varepsilon_\gamma, \tag{10}$$

In this paper, we considered that all elastic moduli of the FGM plate and stiffeners are temperature-dependent. Improved Lekhnitskii's smeared stiffeners technique is obtained by using a transformation technique for stiffeners, force and moment resultants are obtained

$$\begin{Bmatrix}N_x\\N_y\\N_{xy}\\M_x\\M_y\\M_{xy}\end{Bmatrix} = \begin{bmatrix}A_{11}&A_{12}&A_{16}&B_{11}&B_{12}&B_{16}\\A_{12}&A_{22}&A_{26}&B_{12}&B_{22}&B_{26}\\A_{16}&A_{26}&A_{66}&B_{16}&B_{26}&B_{66}\\B_{11}&B_{12}&B_{16}&D_{11}&D_{12}&D_{16}\\B_{12}&B_{22}&B_{26}&D_{12}&D_{22}&D_{26}\\B_{16}&B_{26}&B_{66}&D_{16}&D_{26}&D_{66}\end{bmatrix}\begin{Bmatrix}\varepsilon_x^0\\\varepsilon_y^0\\\gamma_{xy}^0\\-w_{,xx}\\-w_{,yy}\\-w_{,xy}\end{Bmatrix} - \begin{Bmatrix}\phi_0/(1-v)\\\phi_0/(1-v)\\0\\\phi_1/(1-v)\\\phi_1/(1-v)\\0\end{Bmatrix}, \tag{11}$$

with the detail of coefficients $A_{ij}$, $B_{ij}$, $D_{ij}$, $i = (1,2,6)$, $j = (1,2,6)$, $\phi_0$, $\phi_1$ are given in Appendix A.

From the constitutive relations (11), one can write

$$\varepsilon_x^0 = A_{11}^*N_x + A_{12}^*N_y + A_{16}^*N_{xy} + B_{11}^*w_{,xx} + B_{12}^*w_{,yy} + B_{16}^*w_{,xy} + A_{17}^*\frac{\phi_0}{1-v}$$

$$\varepsilon_y^0 = A_{21}^*N_x + A_{22}^*N_y + A_{26}^*N_{xy} + B_{21}^*w_{,xx} + B_{22}^*w_{,yy} + B_{26}^*w_{,xy} + A_{27}^*\frac{\phi_0}{1-v}$$

$$\gamma_{xy}^0 = A_{61}^*N_x + A_{62}^*N_y + A_{66}^*N_{xy} + B_{61}^*w_{,xx} + B_{62}^*w_{,yy} + B_{66}^*w_{,xy} + A_{67}^*\frac{\phi_0}{1-v} \tag{12}$$

in which the detail of coefficients $A_{ij}^*$, $B_{ij}^*$, $i = (1,2,6)$, $j = (1,2,6,7)$ are given in Appendix A.

By substituting Eq. (12) into Eq. (11) leads to

$$\begin{Bmatrix}M_x\\M_y\\M_{xy}\end{Bmatrix} = \begin{Bmatrix}X_{11}&X_{12}&X_{16}&X_{11}^*&X_{12}^*&X_{16}^*\\X_{21}&X_{22}&X_{26}&X_{21}^*&X_{22}^*&X_{26}^*\\X_{61}&X_{62}&X_{66}&X_{61}^*&X_{62}^*&X_{66}^*\end{Bmatrix}\begin{Bmatrix}N_x\\N_y\\N_{xy}\\-w_{,xx}\\-w_{,yy}\\-w_{,xy}\end{Bmatrix} - \begin{Bmatrix}M_x^T\\M_y^T\\M_{xy}^T\end{Bmatrix}, \tag{13}$$

with

$$M_x^T = \frac{\phi_1}{1-v} - (B_{11}A_{17}^* + B_{12}A_{27}^* + B_{16}A_{67}^*)\frac{\phi_0}{1-v},$$

$$M_y^T = \frac{\phi_1}{1-v} - (B_{12}A_{17}^* + B_{22}A_{27}^* + B_{26}A_{67}^*)\frac{\phi_0}{1-v},$$

$$M_{xy}^T = -(B_{16}A_{17}^* + B_{26}A_{27}^* + B_{66}A_{67}^*)\frac{\phi_0}{1-v}. \tag{14}$$

and the Airy's stress function $\varphi(x, y, t)$ is defined as

$$N_x = \frac{\partial^2\varphi}{\partial y^2}, \quad N_y = \frac{\partial^2\varphi}{\partial x^2}, \quad N_{xy} = -\frac{\partial^2\varphi}{\partial x\partial y}. \tag{15}$$

By substituting Eqs. (12), (13) and (15) into Eq. (6) leads to

$$X_{11}^*w_{,xxxx} + (X_{16}^* + 2X_{61}^*)w_{,xxxy} + (X_{12}^* + X_{21}^* + 2X_{66}^*)w_{,xxyy}$$
$$+ (X_{26}^* + 2X_{62}^*)w_{,xyyy}$$
$$+ X_{22}^*w_{,yyyy} - X_{12}\phi_{,xxxx} - (2X_{62} - X_{16})\phi_{,xxxy} - (X_{11} + X_{22} - 2X_{66})\phi_{,xxyy}$$
$$- (2X_{61} - X_{26})\phi_{,xyyy} - X_{21}\phi_{,yyyy} - \phi_{,yy}w_{,xx} + 2\phi_{,xy}w_{,xy} - \phi_{,xx}w_{,yy}$$
$$+ k1w - k_2(w_{,xx} + w_{,yy}) - q = -I_0\frac{\partial^2 w}{\partial t^2} - 2\varepsilon I_0\frac{\partial w}{\partial t} \tag{16}$$

For an imperfect FGM plate, Eq. (16) may be transformed to the form as

$$X_{11}^*w_{,xxxx} + (X_{16}^* + 2X_{61}^*)w_{,xxxy} + (X_{12}^* + X_{21}^* + 2X_{66}^*)w_{,xxyy}$$
$$+ (X_{26}^* + 2X_{62}^*)w_{,xyyy}$$
$$+ X_{22}^*w_{,yyyy} - X_{12}\phi_{,xxxx} - (2X_{62} - X_{16})\phi_{,xxxy} - (X_{11} + X_{22} - 2X_{66})\phi_{,xxyy}$$
$$- (2X_{61} - X_{26})\phi_{,xyyy} - X_{21}\phi_{,yyyy} - \phi_{,yy}(w_{,xx} + w_{,xx}^*) + 2\phi_{,xy}(w_{,xy} + w_{,xy}^*)$$
$$- \phi_{,xx}(w_{,yy} + w_{,yy}^*) + k_1w - k_2(w_{,xx} + w_{,yy}) - q = -I_0\frac{\partial^2 w}{\partial t^2} - 2\varepsilon I_0\frac{\partial w}{\partial t} \tag{17}$$

in which

$$X_{11} = B_{11}A_{11}^* + B_{12}A_{21}^* + B_{16}A_{61}^*, \quad X_{11}^* = D_{11} - (B_{11}B_{11}^* + B_{12}B_{21}^* + B_{16}B_{61}^*)$$

$$X_{12} = B_{11}A_{12}^* + B_{12}A_{22}^* + B_{16}A_{62}^*,$$

$$X_{12}^* = D_{12} - (B_{11}B_{12}^* + B_{12}B_{22}^* + B_{16}B_{62}^*)$$

$$X_{16} = B_{11}A_{16}^* + B_{12}A_{26}^* + B_{16}A_{66}^*,$$

$$X_{16}^* = D_{16} - (B_{11}B_{16}^* + B_{12}B_{26}^* + B_{16}B_{66}^*)$$

$$X_{21} = B_{21}A_{11}^* + B_{22}A_{21}^* + B_{26}A_{61}^*,$$

$$X_{21}^* = D_{12} - (B_{12}B_{11}^* + B_{22}B_{21}^* + B_{26}B_{61}^*)$$

$$X_{22} = B_{21}A_{12}^* + B_{22}A_{22}^* + B_{26}A_{62}^*,$$

$$X_{22}^* = D_{22} - (B_{12}B_{12}^* + B_{22}B_{22}^* + B_{26}B_{62}^*)$$

$$X_{26} = B_{21}A_{16}^* + B_{22}A_{26}^* + B_{26}A_{66}^*,$$

$$X_{26}^* = D_{26} - (B_{12}B_{16}^* + B_{22}B_{26}^* + B_{26}B_{66}^*)$$

$$X_{61} = B_{61}A_{11}^* + B_{62}A_{21}^* + B_{66}A_{61}^*,$$

$$X_{61}^* = D_{16} - (B_{16}B_{11}^* + B_{26}B_{21}^* + B_{66}B_{61}^*)$$

$$X_{62} = B_{61}A_{12}^* + B_{62}A_{22}^* + B_{66}A_{62}^*,$$

$$X_{62}^* = D_{26} - (B_{16}B_{12}^* + B_{26}B_{22}^* + B_{66}B_{62}^*)$$

$$X_{66} = B_{61}A_{16}^* + B_{62}A_{26}^* + B_{66}A_{66}^*,$$

$$X_{66}^* = D_{66} - (B_{16}B_{16}^* + B_{26}B_{26}^* + B_{66}B_{66}^*)$$

$$\tag{18}$$

Introduction of Eq. (12), the Airy's stress function $\varphi(x, y, t)$ into Eq. (5) gives the compatibility equation of the imperfect FGM plate as

$$A_{11}^* \varphi_{,yyyy} - (A_{16}^* + A_{61}^*)\varphi_{,xyyy} + (A_{12}^* + A_{21}^* + A_{66}^*)\varphi_{,xxyy} - (A_{26}^* + A_{62}^*)$$

$$\varphi_{,xxxy} + A_{22}^* \varphi_{,xxxx}$$

$$+ B_{12}^* w_{,yyyy} + (B_{16}^* - B_{62}^*)w_{,xyyy} + (B_{11}^* + B_{22}^* - B_{66}^*)w_{,xxyy} + (B_{26}^* - B_{61}^*)$$

$$w_{,xxxy} + B_{21}^* w_{,xxxx}$$

$$- [(w_{,xy})^2 - w_{,xx}w_{,yy} + 2w_{,xy}w_{,xy}^* - w_{,xx}w_{,yy}^* - w_{,xx}^* w_{,yy}] = 0.$$

$$\tag{19}$$

## 3. Boundary conditions and analytical solutions

An imperfect oblique stiffened FGM plate considered in this paper is assumed to be simply supported and subjected to uniformly distributed pressure of axial compression of intensities $P_x$, respectively, at its cross section.

$$w = M_x = N_{xy} = 0, \quad N_x = N_{x0}, \quad x = 0, a$$

$$w = M_y = N_{xy} = 0, \quad N_y = N_{y0}, \quad y = 0, b.$$

$$\tag{20}$$

The approximate solutions of equations (17) and (19) satisfying the mentioned conditions in equation (20) are chosen in the following from

$$w(x, y, t) = W(t)\sin\lambda_m x \sin\delta_n y, \tag{21}$$

where $\lambda_m = \frac{m\pi}{a}$, $\delta_n = \frac{n\pi}{b}$, $m$, $n = 1,2,3,4...$ are the natural numbers of half waves in the corresponding direction $x$, $y$. $W(t)$ is the time-dependent total amplitude.

Concerning with the initial imperfection $w^*$ we introduce an assumption, it has the form like the plate deflection, i.e.

$$w^*(x, y) = \mu h \sin\lambda_m x \sin\delta_n y, \tag{22}$$

in which $\mu$ is imperfection parameter of the plate.

Introducing Eqs. 21 and 22 into the compatibility equation (19) and solving obtained equation for unknown $\varphi$ leads to

$$\varphi_{(x,y)} = A_1 \cos 2\lambda_m x + A_2 \cos 2\delta_n y + A_3 \sin\lambda_m x \sin\delta_n y$$

$$+ A_4 \cos\lambda_m x \cos\delta_n y + \frac{1}{2}N_{x0}y^2 + \frac{1}{2}N_{y0}x^2.$$

$$\tag{23}$$

with

$$A_1 = \frac{\delta_n^2}{32A_{22}^*\lambda_m^2}W(W + 2\mu h), \quad A_2 = \frac{\lambda_m^2}{32A_{11}^*\delta_n^2}W(W + 2\mu h),$$

$$A_3 = \frac{(Q_1Q_3 - Q_2Q_4)}{Q_1^2 - Q_2^2}W, \quad A_4 = \frac{(Q_1Q_4 - Q_2Q_3)}{Q_1^2 - Q_2^2}W,$$

$$\tag{24}$$

and

$$Q_1 = [A_{11}^*\delta_n^4 + (A_{12}^* + A_{21}^* + A_{66}^*)\lambda_m^2\delta_n^2 + A_{22}^*\lambda_m^4],$$

$$Q_2 = [(A_{16}^* + A_{61}^*)\lambda_m\delta_n^3 + (A_{26}^* + A_{62}^*)\lambda_m^3\delta_n],$$

$$Q_3 = \left[ (B_{26}^* - B_{61}^*)\lambda_m^3\delta_n - B_{21}^*\lambda_m^4 + \left(\frac{1}{a}\lambda_m^2 + \frac{1}{R}\delta_n^2\right) - B_{12}^* \right.$$

$$\left. \delta_n^4 - (B_{11}^* + B_{22}^* - B_{66}^*)\lambda_m^2\delta_n^2 \right],$$

$$Q_4 = (B_{16}^* - B_{62}^*)\lambda_m\delta_n^3. \tag{25}$$

Replacing Eqs. 21–23 into Eq. (17) and then applying Galerkin method to the resulting equations yields

$$l_{11}W + (N_{x0}\lambda_m^2 + N_{y0}\delta_n^2)(W + \mu h) + l_{12}W(W + \mu h) + l_{13}W(W + 2\mu h)$$

$$+ l_{14}W(W + \mu h)(W + 2\mu h) + n_5 q = I_0\frac{\partial^2 W}{\partial t^2} + 2\varepsilon I_0\frac{\partial W}{\partial t}.$$

$$\tag{26}$$

### 3.1. Nonlinear vibration analysis

Nonlinear vibration behavior of plate is investigated by using Runge-Kutta method. Consider a perfect eccentrically oblique stiffened FGM plates ($\mu = 0$), Eq. (26) will be obtained as:

$$I_0 W_{,tt} + 2\varepsilon I_0 W_{,t} + (l_{11} + l_{12})W + l_{13}W^2 + l_{14}W^3 = -l_{15}q, \tag{27}$$

where $l_{ij} = (i = 1, j = 1 \div 5)$ is showed in Appendix.

If the vibration of FGM plates is free and linear, Eq. (27) can be rewritten:

$$I_0 W_{,tt} + (l_{11} + l_{12})W = 0 \tag{28}$$

The equation of nonlinear free vibration of a perfect plate can be obtained from Eq. (28)

$$\omega_{mn} = \sqrt{\frac{-(l_{11} + l_{12})}{I_0}}. \tag{29}$$

### 3.2. Nonlinear dynamic buckling analysis

Assume that the FGM plate is subjected to axial compressive loads $F_x$ uniformly distributed at two curved edges $x = 0$, $a$, in which

$$N_{x0} = -P_x h \tag{30}$$

By substituting Eq. (30) into Eq. (26) leads to

$$P_1 W + P_2(W + \mu h) + P_3 W(W + \mu h) + P_4 W(W + 2\mu h)$$

$$+ P_5 W(W + \mu h)(W + 2\mu h) + P_6 q = I_0\frac{\partial^2 W}{\partial t^2} + 2\varepsilon I_0\frac{\partial W}{\partial t}$$

$$\tag{31}$$

in which the detail of coefficients $P_i$, $i = (1,2,3,4,5,6)$, are given in Appendix.

The nonlinear dynamic response of the eccentrically oblique stiffened FGM plates subjected to uniformly distributed transverse load $q = Q_0 \sin\Omega t$ ($Q_0$ is the amplitude of uniformly excited load, $\Omega$ is the frequency of the load) could be obtained by solving Eq. (31) using fourth order Runge–Kutta method with the initial conditions are chosen as $W(0) = 0$ and $\frac{dW}{dt}(0) = 0$. The dynamic critical load is determined by applying Budiansky–Roth dynamic buckling criterion when external pressure loads varying as linear functions of time, $q = Ct$ ($C$ – a loading speed).

**Table 1**

Comparisons of dimensionless frequency parameter $\varpi = \omega_{mn} h \sqrt{\rho_c / E_c}$ for the FGM plates with the results of Bich et al. [26] and Alijani et al. [31].

| N | Present | Bich et al. [26] | Alijani et al. [31] |
|---|---------|------------------|---------------------|
| 0 | 0.0582 | 0.0597 | 0.0597 |
| 0.5 | 0.0532 | 0.0506 | 0.0506 |
| 1 | 0.0437 | 0.0456 | 0.0456 |
| 4 | 0.0393 | 0.0396 | 0.0396 |
| 10 | 0.0359 | 0.0381 | 0.0380 |

## 4. Numerical results and discussions

### 4.1. Comparison studies

To estimate the accuracy of the method used in this paper, we carry out a comparison with the results of Bich et al. [26] and Alijani et al. [31] for the case of FGM plates as shown in Table 1. As can be observed in Table 1, it is clearly that the result errors are very small so the method in this work is correct and acceptable. Comparison of dynamic critical buckling load of orthogonal stiffened FGM plates with Bich et al. [26] is presented in Table 2. It is also found that the present results agree very well with those of Bich et al. [26].

### 4.2. Nonlinear vibration results

In the section, the components of the material are $Al/Al_2O_3$. The material properties are $E_m = 70\ GPa$, $E_c = 380\ GPa$, $\rho_m = 2702\ kg/m^3$, $\rho_c = 3800\ kg/m^3$. The Poisson ratio is assumed to be $\nu = 0.3$.

Geometric parameters of plate and stiffeners are chosen as $(a/b = 1)$, $b/h = 90$, $s_x = s_y = 0.15(m)$, $z_x = z_y = 0.03(m)$, $\rho_m = 2702\ kg/m^3$, $\rho_c = 3800\ kg/m^3$, $h_x^T = h_y^T = 0.02m$, $d_x^T = d_y^T = 0.008m$.

It can be observed in Table 3, when the elastic foundations parameters increase the natural frequency of plate increases. Table 3 also shows the natural frequencies of the eccentrically stiffened oblique FGM plates are strongly influenced by vibration mode $(m, n)$. The obtained fundamental modes are basic mode $(m,n) = (1,1)$ in all investigated results.

Fig. 2 shows the effect of stiffener angle $(\gamma_1, \gamma_2)$ on the vibration amplitude of FGM plates in 3 cases. Clearly, vibration amplitude of oblique stiffened plates is smaller than one of orthogonal stiffened plates. In case stiffener angle $(\gamma_1 = \pi/4, \gamma_2 = -\pi/4)$, the vibration amplitude of FGM plates are smallest.

The influences of the geometrical properties ($a/b$ and $b/h$ ratios) on the dynamic response of the eccentrically oblique stiffened FGM plates are shown in Figs. 3 and 4. It is obvious that, the ratio $a/b$ or ratio $b/h$ increase the vibration amplitude of eccentrically oblique stiffened FGM plate increases.

Fig. 5 illustrates effect of power law indexes $N = (1,3,5)$ on the of deflection - time curves of the eccentrically oblique stiffened FGM plates with different values $(N)$. The obtained results show that when the power law index increases, the nonlinear vibration amplitude of the

**Table 3**

Effect of vibration modes $(m, n)$ and elastic foundations parameters on the natural frequencies (rad/s) of the eccentrically oblique stiffened FGM plates ($\Delta T = 0K$, $h = 0.01$, $a/h = 90$, $a/b = 1$).

| | Without elastic foundation | $k_1 = 0.3$ (GPa/m); $k_2 = 0.3$ (GPa.m); | $k_1 = 0.6$ (GPa/m); $k_2 = 0.6$ (GPa.m) |
|---|---|---|---|
| $(m,n) = (1,1)$ | 2.8370e+03 | 1.5561e+04 | 2.3137e+04 |
| $(m,n) = (1,2)$ | 3.5056e+03 | 2.4160e+04 | 3.6049e+04 |
| $(m,n) = (1,3)$ | 4.9813e+03 | 3.4036e+04 | 5.0775e+04 |
| $(m,n) = (2,1)$ | 3.5056e+03 | 2.4160e+04 | 3.6049e+04 |
| $(m,n) = (2,2)$ | 6.3301e+03 | 3.0803e+04 | 4.5675e+04 |
| $(m,n) = (2,3)$ | 8.0894e+03 | 3.9197e+04 | 5.8114e+04 |
| $(m,n) = (3,1)$ | 4.9813e+03 | 3.4036e+04 | 5.0775e+04 |
| $(m,n) = (3,2)$ | 8.0894e+03 | 3.9197e+04 | 5.8114e+04 |
| $(m,n) = (3,3)$ | 1.0941e+04 | 4.6399e+04 | 6.8524e+04 |
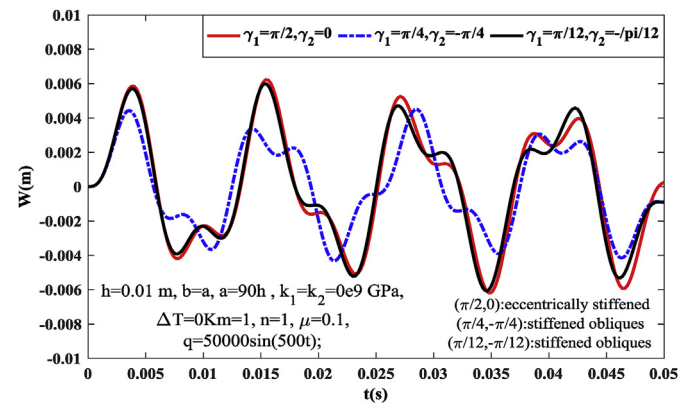


**Fig. 2.** Effect of stiffener angle $\gamma_1$, $\gamma_2$ on the dynamic response of the eccentrically oblique stiffened FGM plates.
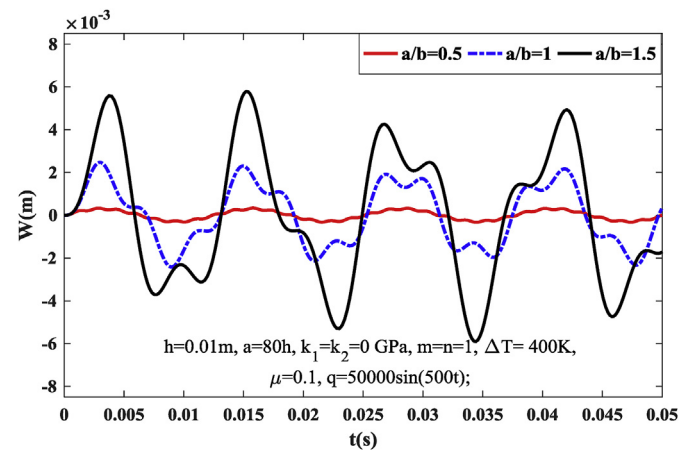


**Fig. 3.** Effect of ratio $a/b$ on the on the deflection - time curves of the eccentrically oblique stiffened FGM plates.

**Table 2**

Comparison of dynamic critical buckling load of orthogonal stiffened FGM plates.

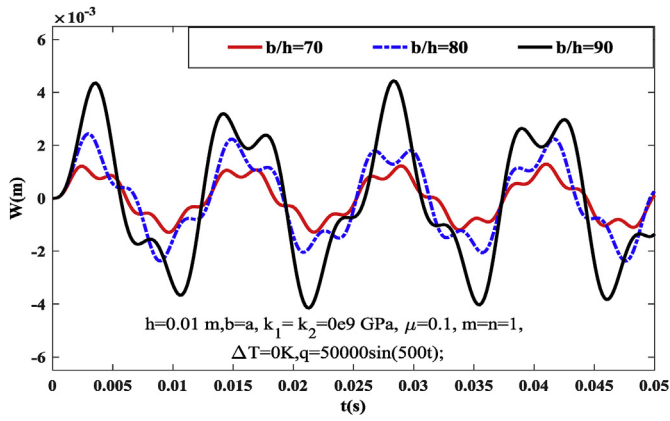| N | Bich et al. [26] | | | Present | | |
|---|---|---|---|---|---|---|
| | Static (m,n) | Dynamic (m,n) | | Static (m,n) | Dynamic (m,n) | |
| | | $c = 1.5 \times 10^9$ | $c = 2 \times 10^9$ | | $c = 1.5 \times 10^9$ | $c = 2 \times 10^9$ |
| 0.2 | 1.350(1,1) | 1.841(1,1) | 1.977(1,1) | 1.350(1,1) | 1.852(1,1) | 1.989(1,1) |
| 1 | 1.155(1,1) | 1.656(1,1) | 1.774(1,1) | 1.155(1,1) | 1.669(1,1) | 1.787(1,1) |
| 5 | 1.031(1,1) | 1.532(1,1) | 1.669(1,1) | 1.031(1,1) | 1.538(1,1) | 1.675(1,1) |
| 10 | 1.024(1,1) | 1.526(1,1) | 1.661(1,1) | 1.024(1,1) | 1.536(1,1) | 1.672(1,1) |

**Fig. 4.** Effect of ratio $b/h$ on the on the deflection - time curves of the eccentrically oblique stiffened FGM plates.
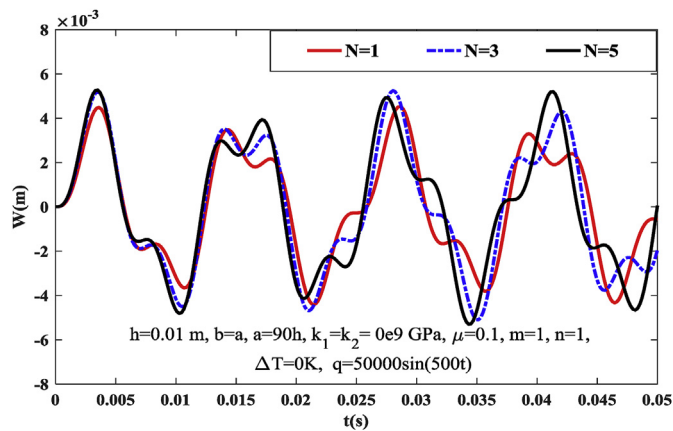


**Fig. 5.** Effect of volume fraction index $N$ on the deflection - time curves of the eccentrically oblique stiffened FGM plates.

eccentrically oblique stiffened FGM plates increases.

Fig. 6 shows the influence of temperature field ($\Delta T = 0$, $\Delta T = 100K$, $\Delta T = 200K$) on the deflection - time curves of the eccentrically stiffened oblique FGM plates. From Fig. 6, can see vibration amplitude of FGM plates increases when we increase value temperature.

Fig. 7 shows the effect of external pressure on the deflection-time curves of the eccentrically oblique stiffened FGM plates with $Q = 30000 (N/m^2)$, $Q = 40000 (N/m^2)$ and $Q = 50000 (N/m^2)$. As can be observed, when the amplitude of external pressure increases, the vibration amplitude of the eccentrically stiffened oblique FGM plates
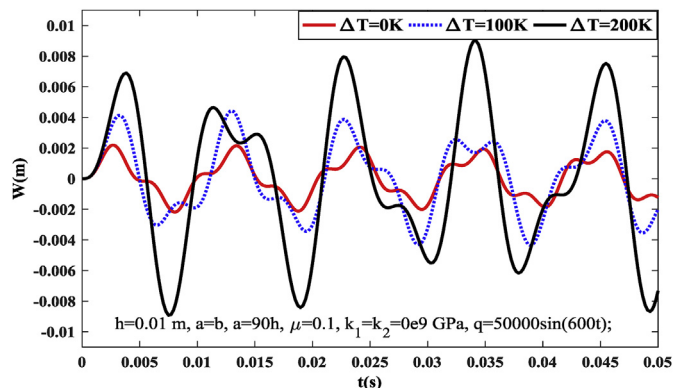


**Fig. 6.** Effect of the temperature field on the deflection - time curves of the eccentrically oblique stiffened FGM plates.
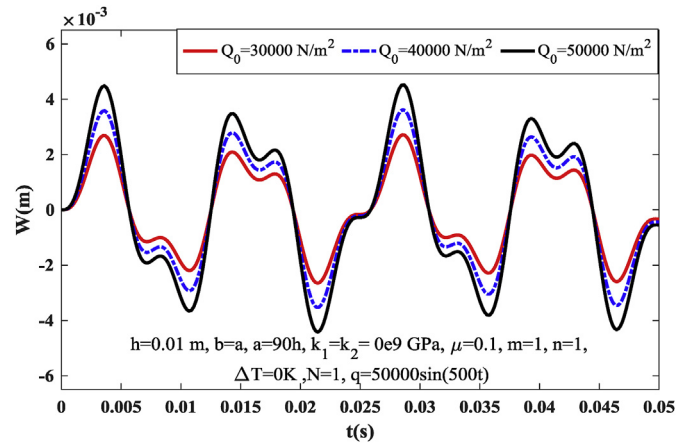


**Fig. 7.** Effect of the external pressure $Q_0$ on the deflection - time curves of the eccentrically oblique stiffened FGM plates.
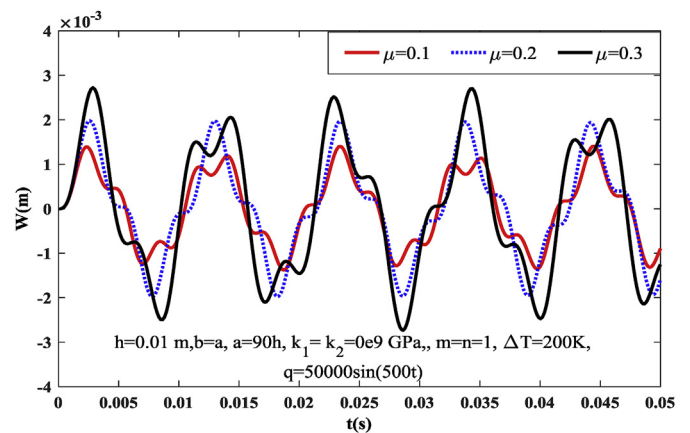


**Fig. 8.** Effect of imperfection $\mu$ on the deflection - time curves of the eccentrically oblique stiffened FGM plates.

strongly increases.

The influence of initial imperfection with amplitude $\mu = (0.1, 0.2, 0.3)$ on the deflection - time curves of the eccentrically oblique stiffened FGM plates is presented in Fig. 8. As expected, the reduction of amplitude of initial imperfection makes the amplitudes of nonlinear vibration of the eccentrically oblique stiffened FGM plate decreases.

### 4.3. Nonlinear dynamic results

Table 4 shows the effects of temperatures change on the nonlinear dynamic response of the eccentrically oblique stiffened FGM plates. Clearly, the critical loads decrease when the temperature change $\Delta T$ increases.

Nonlinear dynamic responses of the eccentrically oblique stiffened FGM plate with different loads are shown in Table 5. As can be seen, the critical loads decrease when the pre-external loads $q$ increases. The

**Table 4**
Effect of temperature change on dynamic critical buckling loads of FGM plate.

|  | $\Delta T$ |  |  |  |  |  |
| --- | --- | --- | --- | --- | --- | --- |
|  | 100K | 200K | 400K | 500K | 700K | 900K |
| $P_x = 3.5 \times 10^{11}t$ | 5.236 | 5.019 | 4.578 | 4.379 | 3.948 | 3.511 |
| $P_x = 5.0 \times 10^{11}t$ | 5.490 | 5.285 | 4.834 | 4.641 | 4.213 | 3.775 |
| $P_x = 7.5 \times 10^{11}t$ | 5.894 | 5.678 | 5.237 | 5.028 | 4.609 | 4.170 |

**Table 5**
Dynamic critical buckling of the eccentrically oblique stiffened FGM plate with different loads.

| | $q$ | | | | | |
|---|---|---|---|---|---|---|
| | $10^5$ | $3 \times 10^5$ | $5 \times 10^5$ | $7 \times 10^5$ | $9 \times 10^5$ | $2 \times 10^6$ |
| $P_x = 3.5 \times 10^{11}t$ | 4.781 | 4.757 | 4.718 | 4.690 | 4.666 | 4.596 |
| $P_x = 5.0 \times 10^{11}t$ | 5.040 | 5.000 | 4.966 | 4.939 | 4.914 | 4.828 |
| $P_x = 7.5 \times 10^{11}t$ | 5.431 | 5.415 | 5.353 | 5.315 | 5.294 | 5.177 |
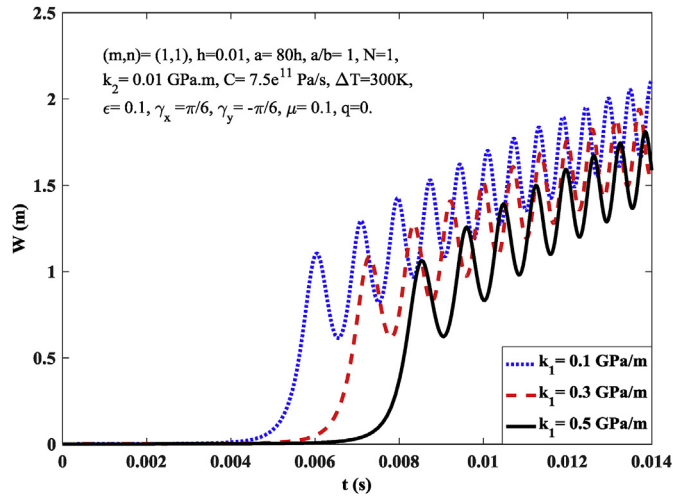


**Fig. 9.** Effect of the linear Winkler foundation on the nonlinear vibration and dynamic response of eccentrically oblique stiffened FGM plate.

dynamic buckling load increase when loading speed increases.

Figs. 9 and 10 show the effects of elastic foundations on the non-linear dynamic stability of the eccentrically oblique stiffened FGM plate with immovable edges under uniform external pressure. Obviously, the dynamic critical buckling loads of the plate become considerably higher due to the support of elastic foundations. In addition, the beneficial effect of the Pasternak foundation on the buckling of the eccentrically oblique stiffened FGM plate is better than the Winkler one.

Fig. 11 analyzes the effects of geometrical parameters on the non-linear static and dynamic stability of eccentrically oblique stiffened FGM plate. Specifically, Fig. 11 illustrates the effect of ratio $b/a$ on the nonlinear static stability eccentrically oblique stiffened FGM plate with
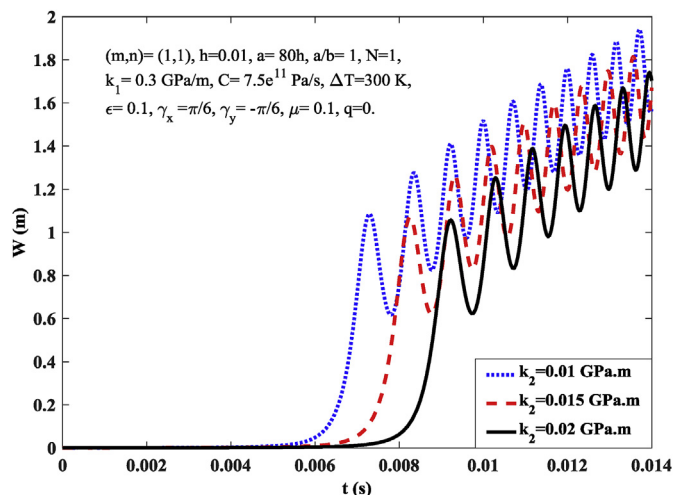


**Fig. 10.** Effect of the Pasternak foundation on the nonlinear vibration and dynamic response of eccentrically oblique stiffened FGM plate.
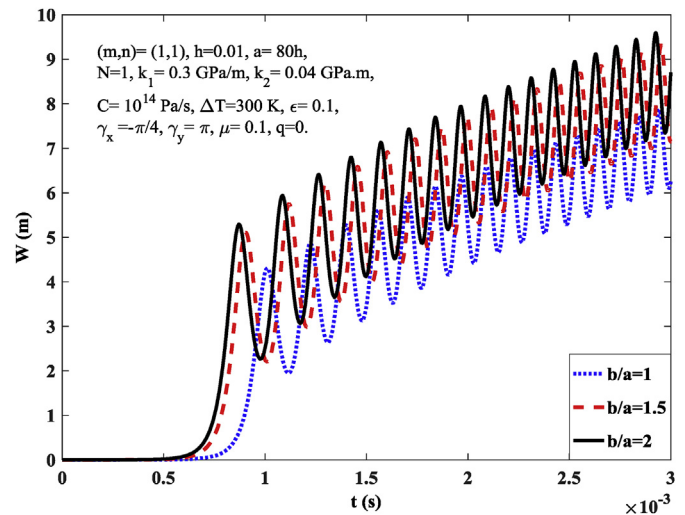


**Fig. 11.** Effect of ratio $b/a$ on the nonlinear vibration and dynamic response of eccentrically oblique stiffened FGM plate.
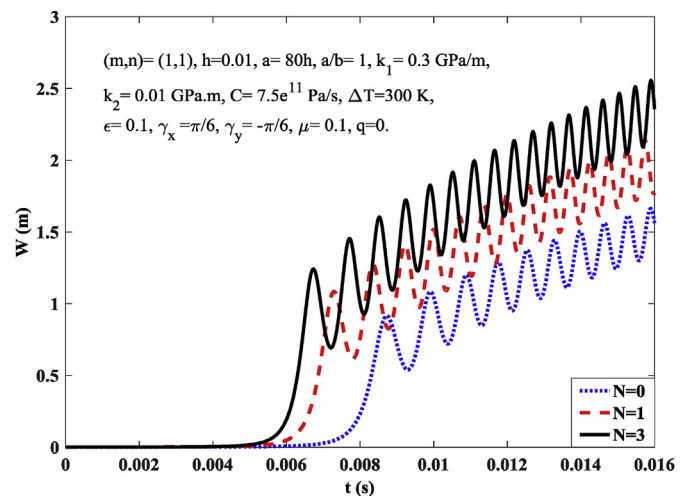


**Fig. 12.** Effect of volume fraction index $N$ on the nonlinear vibration and dynamic response of eccentrically oblique stiffened FGM plate.

movable edges under uniform external pressure. Furthermore, the dynamic critical load of the FGM plate increases when the ratio $b/a$ decreases.

Fig. 12 presents the effect of volume fraction index $N$ on the nonlinear dynamic response of eccentrically oblique stiffened FGM plate with $\Delta T = 300K$, $a.b = 1$, $\mu = 0.1$, $\gamma_x = \pi/6$, $\gamma_y = -\pi/6$. It can be seen that the dynamic critical load of the nonlinear dynamic response of eccentrically stiffened FGM plate increases when increasing the volume fraction index $N$.

Fig. 13 illustrates the effect of initial imperfection on the nonlinear vibration and dynamic response of eccentrically oblique stiffened FGM plate. Obviously, the dynamic critical load will decrease and loses the stability if the initial imperfection increases. As can be seen, the imperfect coefficient has a significant effect on the dynamic response of the eccentrically oblique stiffened FGM plate.

Figs. 14–15 indicate the effects of stiffener angle on the nonlinear dynamic response of eccentrically oblique stiffened FGM plate. Obviously, the dynamic critical load maximum value when $\gamma_x = \pi/4$.

Fig. 16 describes the nonlinear dynamic responses of the eccentrically oblique stiffened FGM plate with different loads. We can see that the dynamic critical load will decrease and if the initial imperfection increases.
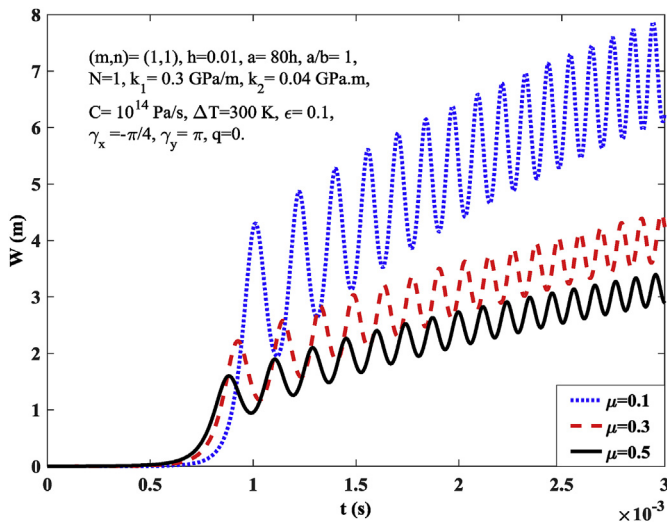
**Fig. 13.** Effect of initial imperfection on the nonlinear vibration and dynamic response of eccentrically oblique stiffened FGM plate.
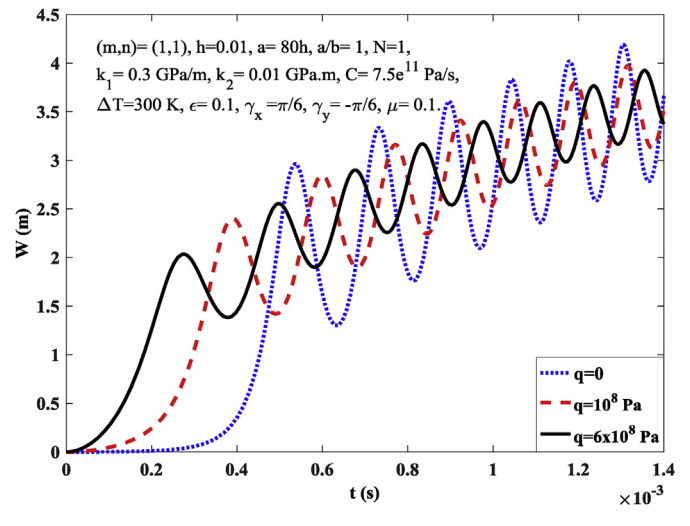


**Fig. 14.** Effect of stiffeners angle on the nonlinear dynamic response of eccentrically oblique stiffened FGM plate.



**Fig. 15.** Comparison critical dynamic load between eccentrically orthogonal stiffened and eccentrically oblique stiffened.



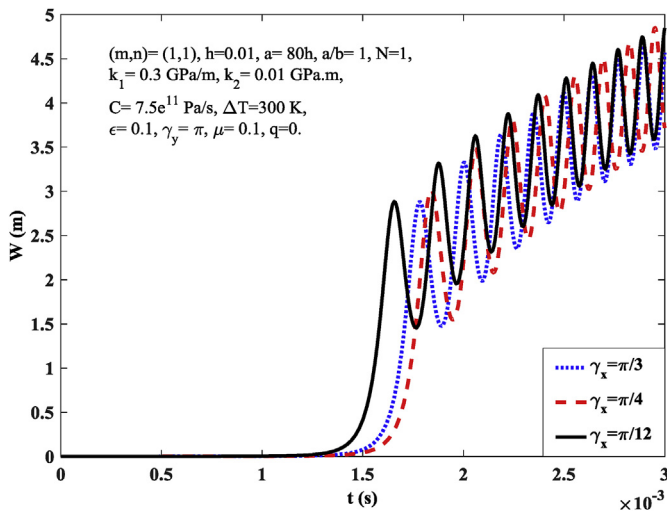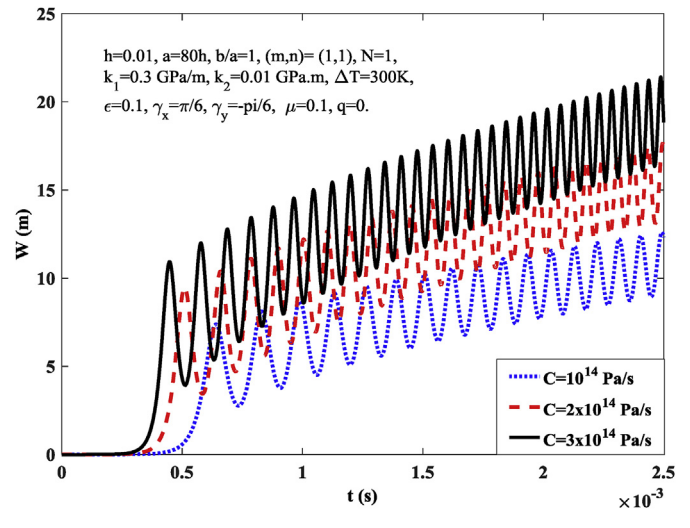**Fig. 16.** Nonlinear dynamic responses of the eccentrically oblique stiffened FGM plate with different loads.



**Fig. 17.** Effect of the loading speed $C$ on the nonlinear dynamic response of eccentrically oblique stiffened FGM plate.

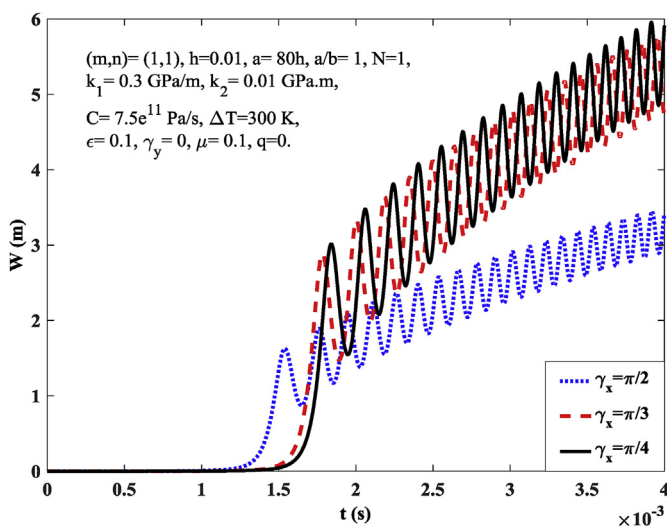Fig. 17. Shows the effects of the loading speed $C$ on the dynamic response of eccentrically oblique stiffened FGM plate. The results show that the value of the critical load increases when the loading speed increases.

## 5. Conclusions

This is the paper presents a semi-analytical approach to investigate the nonlinear vibration and dynamic buckling of eccentrically oblique stiffened FGM plate resting on elastic foundation in thermal environment by using of the classical plate theory. Numerical results for dynamic response of the eccentrically oblique stiffened thin FGM plates are obtained by Galerkin method, stress function and improved Lekhnitskii's smeared stiffeners technique. From the obtained results in this paper, we can conclude that

- The initial imperfection has a significant influence on the nonlinear vibration and dynamic response of eccentrically oblique stiffened FGM plate.
- The oblique stiffener system strongly enhances the load-carrying capacity of the eccentrically stiffened thin FGM plates in comparison with orthogonal stiffener.

- The pre-loaded axial compressions strongly influence on the critical dynamic response of the stiffened plate.
- The elastic foundations and temperature have a strong effect on the nonlinear dynamic response of the thin FGM plates and the beneficial effect of the Pasternak foundation is better than the Winkler one, and the critical dynamic load of the plate decreases when the temperature increases.

## Acknowledgements

## Appendix

$$B_{26} = \frac{E_0 A_x^T}{s_x^T} e_i^T (\sin^3 \gamma_x \cos \gamma_x + \sin^3 \gamma_y \cos \gamma_y),$$

$$B_{66} = \overline{B_{66}} + \frac{E_0 A_x^T}{s_x^T} e_i^T (\sin^2 \gamma_x \cos^2 \gamma_x + \sin^2 \gamma_y \cos^2 \gamma_y),$$

$$D_{11} = \overline{D_{11}} + \frac{E_0 A_y^T}{s_y^T} (\cos^4 \gamma_x + \cos^4 \gamma_y), \quad D_{12} = \overline{D_{12}} + \frac{E_0 A_y^T}{s_y^T} (\sin^2 \gamma_x \cos^2 \gamma_x + \sin^2 \gamma_y \cos^2 \gamma_y),$$

$$D_{22} = \overline{D_{22}} + \frac{E_0 A_y^T}{s_y^T} (\sin^4 \gamma_x + \sin^4 \gamma_y), \quad D_{16} = \frac{E_0 A_y^T}{s_y^T} (\sin \gamma_x \cos^3 \gamma_x + \sin \gamma_y \cos^3 \gamma_y),$$

$$D_{26} = \frac{E_0 A_y^T}{s_y^T} (\sin^3 \gamma_x \cos \gamma_x + \sin^3 \gamma_y \cos \gamma_y),$$

$$D_{66} = \overline{D_{66}} + \frac{E_0 A_y^T}{s_y^T} (\sin^2 \gamma_x \cos^2 \gamma_x + \sin^2 \gamma_y \cos^2 \gamma_y),$$

$$\overline{A_{11}} = \overline{A_{22}} = \frac{E_1}{1 - \nu^2}, \quad \overline{A_{12}} = \nu \overline{A_{11}}, \quad \overline{A_{66}} = \frac{E_1}{2(1+\nu)}, \quad \overline{D_{11}} = \overline{D_{11}} = \frac{E_3}{1 - \nu^2}, \quad \overline{D_{12}} = \nu \overline{D_{11}}, \quad \overline{D_{66}} = \frac{E_3}{2(1+\nu)},$$

$$\overline{B_{11}} = \overline{B_{11}} = \frac{E_2}{1 - \nu^2}, \quad \overline{B_{12}} = \nu \overline{B_{11}}, \quad \overline{B_{66}} = \frac{E_2}{2(1+\nu)},$$

$$\Delta = A_{11} A_{22} A_{66} - A_{11} A_{26} A_{62} - A_{16} A_{22} A_{61} - A_{12} A_{21} A_{66} + A_{12} A_{26} A_{61} + A_{16} A_{21} A_{62}$$

$$A_{11}^* = \frac{(A_{22} A_{66} - A_{26} A_{62})}{\Delta}, A_{12}^* = \frac{(A_{16} A_{62} - A_{12} A_{66})}{\Delta}, A_{16}^* = \frac{(A_{12} A_{26} - A_{16} A_{22})}{\Delta},$$

$$A_{17}^* = A_{11}^* + A_{12}^*, \quad B_{11}^* = A_{11}^* B_{11} + A_{12}^* B_{21} + A_{16}^* B_{16},$$

$$B_{12}^* = A_{11}^* B_{12} + A_{12}^* B_{22} + A_{16}^* B_{62}, \quad B_{16}^* = A_{11}^* B_{16} + A_{12}^* B_{26} + A_{16}^* B_{66},$$

$$A_{21}^* = \frac{(A_{26} A_{61} - A_{21} A_{66})}{\Delta}, A_{22}^* = \frac{(A_{11} A_{66} - A_{16} A_{61})}{\Delta}, A_{26}^* = \frac{(A_{16} A_{21} - A_{11} A_{26})}{\Delta},$$

$$A_{27}^* = A_{21}^* + A_{22}^*, \quad B_{21}^* = A_{21}^* B_{11} + A_{22}^* B_{21} + A_{26}^* B_{16},$$

$$B_{22}^* = A_{21}^* B_{12} + A_{22}^* B_{22} + A_{26}^* B_{62}, \quad B_{26}^* = A_{21}^* B_{16} + A_{22}^* B_{26} + A_{26}^* B_{66},$$

$$A_{61}^* = \frac{A_{21} A_{62} - A_{22} A_{61}}{\Delta}, A_{62}^* = \frac{A_{12} A_{61} - A_{11} A_{62}}{\Delta}, A_{66}^* = \frac{A_{11} A_{22} - A_{12} A_{21}}{\Delta}, A_{67}^* = A_{61}^* + A_{62}^*,$$

$$B_{61}^* = B_{11} A_{61}^* + B_{21} A_{62}^* + B_{61} A_{66}^*, \quad B_{62}^* = B_{12} A_{61}^* + B_{22} A_{62}^* + B_{62} A_{66}^*, \quad B_{66}^* = B_{16} A_{61}^* + B_{26} A_{62}^* + B_{66} A_{66}^*.$$

$$E_1 = E_m h + E_{cm} h/(k+1), \quad E_2 = E_{cm} h^2 [1/(k+2) - 1/(2k+2)],$$

$$E_3 = E_m h^3/12 + E_{cm} h^3 [1/(k+3) - 1/(k+2) + 1/(4k+4)],$$

$$(\phi_o, \phi_1) = \int_{-h/2}^{h/2} \left[ E_m + E_{cm} \left( \frac{2z+h}{2h} \right)^k \right] \left[ \alpha_m + \alpha_{cm} \left( \frac{2z+h}{2h} \right)^k \right] \Delta T (1, z) dz.$$

$$l_{11} = - \left\{ \begin{array}{l} (X_{11}^* \lambda_m^4 + X_{22}^* \delta_n^4) - (X_{16}^* + 2X_{61}^*) \lambda_m^3 \delta_n + (X_{12}^* + X_{21}^* + 2X_{66}^*) \lambda_m^2 \delta_n^2 \\ -[X_{12} \lambda_m^4 + X_{21} \delta_n^4 + (X_{11} + X_{22} - 2X_{66}) \lambda_m^2 \delta_n^2] \frac{(Q_1 Q_3 - Q_2 Q_4)}{Q_1^2 - Q_2^2} \\ +[(2X_{62} - X_{16}) \lambda_m^2 + (2X_{61} - X_{26}) \delta_n^2] \lambda_m \delta_n \frac{(Q_1 Q_4 - Q_2 Q_3)}{Q_1^2 - Q_2^2} \\ +k_1 + k_2 (\lambda_m^2 + \delta_n^2) \end{array} \right\},$$

$$l_{12} = \frac{32 \lambda_m \delta_n}{3ab} \frac{(Q_1 Q_3 - Q_2 Q_4)}{Q_1^2 - Q_2^2},$$

$$l_{13} = -\frac{2}{3ab} \left[ \begin{array}{l} \frac{\delta_n}{\lambda_m^3 A_{22}^*} (4X_{12} \lambda_m^4) \\ + \frac{\lambda_m}{\delta_n^3 A_{11}^*} (4X_{21} \delta_n^4) \end{array} \right], \quad l_{14} = -\frac{1}{16} \left( \frac{\lambda_m^4}{A_{11}^*} + \frac{\delta_n^4}{A_{22}^*} \right), \quad n_5 = \frac{16}{mn\pi^2},$$

$$n_1 = -\frac{4}{mn\pi^2} \left[ (A_{21}^* \delta_n^2 + A_{22}^* \lambda_m^2) \frac{(Q_1 Q_3 - Q_2 Q_4)}{Q_1^2 - Q_2^2} + A_{26}^* \lambda_m \delta_n \frac{(Q_1 Q_4 - Q_2 Q_3)}{Q_1^2 - Q_2^2} + (B_{21}^* \lambda_m^2 + B_{22}^* \delta_n^2) \right],$$

$$m_1 = -\frac{n_1}{A_{22}^*}, \quad m_2 = \frac{\delta_n^2}{8 A_{22}^*}, \quad m_3 = -\left( \frac{A_{21}^*}{A_{22}^*} N_{x0} + \frac{A_{27}^*}{A_{22}^*} \frac{\phi_0}{1 - \nu} \right),$$

$P_1 = -l_{11}, \quad P_2 = -(-P_x h \lambda_m^2 + m_3 \delta_n^2),$

$P_3 = -(m_1 \delta_n^2 + l_{12}), \quad P_4 = -l_{13}, \quad P_5 = -(m_2 \delta_n^2 + l_{14}),$

$P_6 = -n_5.$

# References

[1] G.N. Praveen, C.D. Chin, J.N. Reddy, Thermoelastic analysis of functionally graded ceramic-metal cylinder, Journal of Engineering Mechanics ASCE 125 (1999) 1259–1267.

[2] G.N. Praveen, J.N. Reddy, Nonlinear transient thermoelastic analysis of functionally graded ceramic-metal plates, Int. J. Solids Struct. 35 (1998) 4457–4476.

[3] J.N. Reddy, Analysis of functionally graded plates, Int. J. Numer. Methods Eng. 47 (2000) 663–684.

[4] J.N. Reddy, C.D. Chin, Thermomechanical analysis of functionally graded cylinders and plates, J. Therm. Stress. 21 (1998) 593–626.

[5] R.A. Arciniega, J.N. Reddy, Large deformation analysis of functionally graded shells, Int. J. Solids Struct. 44 (2007) 2036–2052.

[6] L.S. Ma, T.J. Wang, Nonlinear bending and post-buckling of a functionally graded circular plate under mechanical and thermal loadings, Int. J. Solids Struct. 40 (2003) 3311–3330.

[7] H. Matsunaga, Stress analysis of functionally graded plates subjected to thermal mechanical loadings, Compos. Struct. 87 (2009) 344–357.

[8] R. Javaheri, M.R. Eslami, Buckling of functionally graded plates under in-plane compressive loading, J. Appl. Math. Mech. ZAMM 82 (2002) 277–283.

[9] R. Javaheri, M.R. Eslami, Thermal buckling of functionally graded plates, AIAA J. 40 (1) (2002) 162–169.

[10] R. Javaheri, M.R. Eslami, Thermal buckling of functionally graded plates based on higher order theory, J. Therm. Stress. 25 (2002) 603–625.

[11] B.A. Samsam Shariat, M.R. Eslami, Buckling of thick functionally graded plates under mechanical and thermal loads, Compos. Struct. 78 (2007) 433–439.

[12] B.A. Samsam Shariat, M.R. Eslami, Effect of initial imperfection on thermal buckling of functionally graded plates, J. Therm. Stress. 28 (2005) 1183–1198.

[13] B.A. Samsam Shariat, R. Javaheri, M.R. Eslami, Buckling of imperfect functionally graded plates under in-plane compressive loading, Thin-Walled Struct. 43 (2005) 1020–1036.

[14] B.A. Samsam Shariat, M.R. Eslami, Thermal buckling of imperfect functionally graded plates, Int. J. Solids Struct. 43 (2006) 4082–4096.

[15] W. Lanhe, Thermal buckling of a simply supported moderately thick rectangular FGM plate, Compos. Struct. 64 (2004) 211–218.

[16] F. Ebrahimi, A. Rastgoo, A.A. Atai, A theoretical analysis of smart moderately thick shear deformable annular functionally graded plate, Eur. J. Mech. A Solid. 28 (2009) 962–973.

[17] M. Taczała, R. Buczkowski, M. Kleiber, Nonlinear buckling and post-buckling response of stiffened FGM plates in thermal environments, Compos. B Eng. 109 (2017) 238–247.

[18] Y.Q. Wang, J.W. Zu, Nonlinear steady-state responses of longitudinally traveling functionally graded material plates in contact with liquid, Compos. Struct. 164 (2017) 130–144.

[19] Y.Q. Wang, J.W. Zu, Nonlinear dynamic thermoelastic response of rectangular FGM plates with longitudinal velocity, Compos. B Eng. 117 (2017) 74–88.

[20] Y.Q. Wang, J.W. Zu, Large-amplitude vibration of sigmoid functionally graded thin plates with porosities, Thin-Walled Struct. 119 (2017) 911–924.

[21] Y.Q. Wang, J.W. Zu, Nonlinear dynamics of a translational FGM plate with strong mode interaction, Int. J. Struct. Stab. Dyn. 18 (2018) 1850031.

[22] Y.Q. Wang, Electro-mechanical vibration analysis of functionally graded piezo-electric porous plates in the translation state, Acta Astronaut. 143 (2018) 263–271.

[23] Y.Q. Wang, J.W. Zu, Porosity-dependent nonlinear forced vibration analysis of functionally graded piezoelectric smart material plates, Smart Mater. Struct. 26 (2017) 105014.

[24] Y.Q. Wang, J.W. Zu, Vibration behaviors of functionally graded rectangular plates with porosities and moving in thermal environment, Aero. Sci. Technol. 69 (2017) 550–562.

[25] Y.Q. Wang, Z. Yang, Nonlinear vibrations of moving functionally graded plates containing porosities and contacting with liquid: internal resonance, Nonlinear Dynam. 90 (2017) 1461–1480.

[26] D.H. Bich, D.V. Dung, V.H. Nam, Nonlinear dynamical analysis of eccentrically stiffened functionally graded cylindrical panels, Compos. Struct. 94 (2012) 2465–2473.

[27] N.D. Duc, P.T. Thang, Nonlinear dynamic response and vibration of shear deformable imperfect eccentrically stiffened S-FGM circular cylindrical shells surrounded on elastic foundations, Aero. Sci. Technol. 40 (2015) 115–127.

[28] N.D. Duc, N.D. Tuan, P. Tran, P.H. Cong, P.D. Nguyen, Nonlinear stability of eccentrically stiffened S-FGM elliptical cylindrical shells in thermal environment, Thin-Walled Struct. 108 (2016) 280–290.

[29] N.D. Duc, P.H. Cong, Nonlinear thermal stability of eccentrically stiffened functionally graded truncated conical shells surrounded on elastic foundations, Eur. J. Mech. A Solid. 50 (2015) 120–131.

[30] N.D. Duc, P.H. Cong, N.D. Tuan, P. Tran, V.M. Anh, V.D. Quang, Nonlinear vibration and dynamic response of imperfect eccentrically stiffened shear deformable sandwich plate with functionally graded material in thermal environment, J. Sandw. Struct. Mater. 18 (2016) 445–473.

[31] F. Alijani, M. Amabili, K. Karagiozis, F. Bakhtiari-Nejad, Nonlinear vibrations of functionally graded doubly curved shallow shells, J. Sound Vib. 330 (2011) 1432–1454.

[32] R. Kolahchi, M. Safari, E. Masoud, Dynamic stability analysis of temperature-dependent functionally graded CNT-reinforced visco-plates resting on orthotropic elastomeric medium, Compos. Struct. 150 (2016) 255–265.

[33] R. Kolahchi, A. Cheraghbak, Agglomeration effects on the dynamic buckling of viscoelastic microplates reinforced with SWCNTs using Bolotin method, Nonlinear Dynam. 90 (2017) 479–492.

[34] R. Kolahchi, A comparative study on the bending, vibration and buckling of viscoelastic sandwich nano-plates based on different nonlocal theories using DC, HDQ and DQ methods, Aero. Sci. Technol. 66 (2017) 235–248.

[35] Y.Q. Wang, Nonlinear vibration of a rotating laminated composite circular cylindrical shell: traveling wave vibration, Nonlinear Dynam. 77 (2014) 1693–1707.

[36] Y.Q. Wang, C. Ye, J.W. Zu, Nonlinear vibration of metal foam cylindrical shells reinforced with graphene platelets, Aero. Sci. Technol. 85 (2019) 359–370.

[37] Y.Q. Wang, Y.H. Wan, J.W. Zu, Nonlinear dynamic characteristics of functionally graded sandwich thin nanoshells conveying fluid incorporating surface stress influence, Thin-Walled Struct. 135 (2019) 537–547.

[38] D.D. Brush, B.O. Almroth, Buckling of Bars, Plates and Shells, Mc. Graw-Hill, 1975.